

UC Irvine

UC Irvine Previously Published Works

Title

Physical mechanisms controlling the generation of laser-induced stresses

Permalink

<https://escholarship.org/uc/item/9zz8d2t7>

ISBN

9780819411099

Authors

Venugopalan, Vasan
Zweig, AD
Deutsch, Thomas F
et al.

Publication Date

1993-07-07

DOI

10.1117/12.147650

Copyright Information

This work is made available under the terms of a Creative Commons Attribution License, available at <https://creativecommons.org/licenses/by/4.0/>

Peer reviewed

PHYSICAL MECHANISMS CONTROLLING THE GENERATION OF LASER-INDUCED STRESSES

V. Venugopalan*[†], A. D. Zweig*, T. F. Deutsch*, N. S. Nishioka*, and B. B. Mikić[†]*Wellman Laboratories of Photomedicine, Department of Dermatology,
Harvard Medical School, Massachusetts General Hospital, Boston, MA 02114

and

[†]Department of Mechanical Engineering, Massachusetts Institute of Technology, Cambridge, MA 02139.**Abstract**

The mechanisms responsible for the generation of stresses by pulsed-laser energy deposition in solids are elucidated with special attention given to laser-tissue interactions. These mechanisms include thermal expansion, subsurface cavity formation, ablative recoil and plasma formation and expansion. Scaling laws are presented for the magnitude of the stresses generated by each of these processes. The effect of laser parameters and material properties on the magnitude and temporal behavior of the stress transients is considered. The use of these scaling laws in conjunction with measurement of stress transients produced by pulsed laser sources may be a powerful tool in determining the physical processes which control the response of materials to pulsed energy deposition. In addition, the controlled generation and accurate measurement of acoustic transients may have important diagnostic and therapeutic applications.

1 Introduction

Pulsed lasers are frequently used as tools for the precise incision and excision of biological tissue. The stress transients generated within the tissue as a result of pulsed laser heating and ablation are receiving increased attention for their potential therapeutic and destructive effects [3, 6]. In addition, the measurement of the stresses resulting from pulsed heating of tissue is proving to be a valuable research tool in investigating the dynamics of laser ablation [5, 4]. However, even with this interest in laser-induced stresses in tissue, no clear framework has been established to predict the nature of these stresses.

The objective of this paper is two fold. First, we will describe some of the physical mechanisms responsible for the optical generation of stresses. Second, we will predict the magnitude and duration of the stress transients associated with these mechanisms. Emphasis is placed on the development of scaling laws which relate the characteristics of the stress transients to laser and material parameters. Once these scaling laws are understood, experiments can be designed to discriminate between physical mechanisms that may be operative in a given laser-target interaction.

2 Thermoelastic Stress Generation

In most instances the thermoelastic effect is the dominant mechanism of stress generation in cases where energy deposition results solely in heating and thermal expansion of the medium. For a linearly elastic isotropic solid with constant thermophysical properties, the equation of motion in one-dimension takes the form [13]:

$$\left(\kappa + \frac{4}{3}\mu\right) \frac{\partial^2 u}{\partial x^2} - 3\beta\kappa \frac{\partial(T - T_\infty)}{\partial x} = \rho \frac{\partial^2 u}{\partial t^2} \quad (1)$$

where

t – time, [s].

T – temperature, [K].

T_∞ – initial temperature, [K],

u – particle displacement, [m].

x – depth within the target, [m].

β – coefficient of thermal expansion, [K⁻¹],

κ – bulk modulus, [Pa].

μ – shear modulus, [Pa] and

ρ – tissue density, [kg m⁻³].

The first term in eqn. (1) represents the spatial gradient of internal stresses within the medium, the second represents the spatial gradient of stresses produced by thermal expansion of the medium and the last represents the net particle acceleration produced by the stress gradients.

For the cases we consider, the temperature rise results from the absorption of laser energy by the tissue. Assuming that Beer's law governs the absorption of the laser radiation, eqn. (1) takes the form:

$$\left(\kappa + \frac{4}{3}\mu\right) \frac{\partial^2 u}{\partial x^2} - \Gamma\mu_a \frac{\partial \varepsilon''(x,t)}{\partial x} = \rho \frac{\partial^2 u}{\partial t^2}, \quad (2)$$

where $\Gamma = 3\beta\kappa/\rho c_v$ is the Grüneisen coefficient and $\varepsilon''(x,t) = \int_{-\infty}^t (1-R)q''(t') \exp(-\mu_a x) dt'$ is the total radiant exposure deposited up to time t , q'' being the incident irradiance, R the surface reflectivity and μ_a the optical absorption coefficient. If the target surface is free, stresses that move towards the surface are reflected back with a change in sign and results in a bipolar stress transient. In this case the initial and boundary conditions necessary to solve eqn. (2) are:

$$u|_{(x,t \rightarrow -\infty)} = \frac{\partial u}{\partial t}|_{(x,t \rightarrow -\infty)} = 0, \quad (3)$$

$$u|_{(x=0^-,t)} = u|_{(x=0^+,t)} \quad (4)$$

and

$$\left(\kappa + \frac{4}{3}\mu\right) \frac{\partial u}{\partial x}|_{(x=0^+,t)} - 3\beta\kappa [T|_{(x=0^+,t)} - T_\infty] = 0. \quad (5)$$

Eqn. (3) requires that the medium be at rest and stress free as time approaches $-\infty$. Eqns. (4) and (5) require that the particle displacement and stress be continuous across the free surface. The solution to eqns. (2)–(5) with these conditions can be found in [2].

To derive the appropriate scaling laws we consider the situation shown in figure 1 where laser radiation of irradiance q'' and duration t_p is incident on the free surface of an absorbing medium with absorption coefficient μ_a . We wish to characterize the stress transient measured by a stress measurement device located at a depth $\delta \gg \mu_a^{-1}$. To do this, consider a layer of infinitesimal thickness $d\lambda$ located at a depth λ where $d\lambda/2 \leq \lambda \ll \delta$. The total energy absorbed by this layer at a given time t is $\int_{-\infty}^t \mu_a q''(t') \exp(-\mu_a \lambda) d\lambda dt'$. The absorption of the laser energy by the layer launches two compressive stress transients, one moving towards the free surface $\sigma_{xx}^-(t)$ and the other moving into the bulk of the solid $\sigma_{xx}^+(t)$. Since the stress which travels towards the free surface gets reflected with a change of sign, the measured stress is given by:

$$\sigma_{xx}(x = \delta, t) = \int_0^\delta \left[\int_{-\infty}^{t - [(\delta - \lambda)/c]} \sigma_{xx}^+(\lambda, t') dt' - \int_{-\infty}^{t - [(\delta + \lambda)/c]} \sigma_{xx}^-(\lambda, t') dt' \right] d\lambda, \quad (6)$$

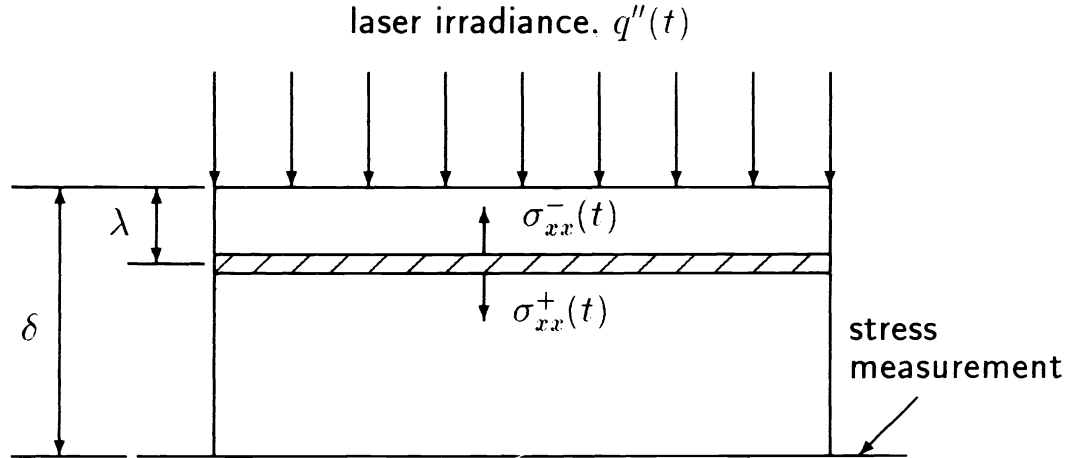


Figure 1: Measurement of acoustic transients generated by pulsed energy deposition in an absorbing medium. See text for details.

where $c = [(\kappa + 4\mu/3)/\rho]^{1/2}$, the propagation velocity of an acoustic wave. Alternatively, the measured stress can be expressed in terms of the laser the energy deposition:

$$\sigma_{xx}(x = \delta, t) = \int_0^\delta \frac{\Gamma}{2} \mu_a \exp(-\mu_a \lambda) \left[\int_{-\infty}^{t - [(\delta - \lambda)/c]} q''(t') dt' - \int_{-\infty}^{t - [(\delta + \lambda)/c]} q''(t') dt' \right] d\lambda. \quad (7)$$

We define a new variable $\xi = t' - \{t - [(\delta - \lambda)/c]\}$ which allows eqn. (7) to be written more simply as:

$$\sigma_{xx}(x = \delta, t) = \int_0^\delta \left[\frac{\Gamma}{2} \mu_a \exp(-\mu_a \lambda) \int_0^{2\lambda/c} q'' \left(\xi + t - \frac{\delta + \lambda}{c} \right) d\xi \right] d\lambda. \quad (8)$$

In eqn. (8), we see that only the energy deposited in the time interval $0 \leq t \leq 2\lambda/c$ contributes to the measured stress. Since the characteristic length scale in this process is the absorption depth $\lambda = \mu_a^{-1}$ we should consider those cases where the laser pulse duration, t_p is much smaller or much larger than the characteristic time $1/\mu_a c$. In the limiting case where the laser pulse duration is much shorter than the acoustic transit time, i.e., $\mu_a c t_p \ll 1$, significant particle motion occurs only after the laser pulse. Accordingly, there is no relaxation of the stresses developed in the heated layer during the laser pulse. Thus the magnitude of the stresses scales with the volumetric energy deposition $\mu_a \varepsilon''$ and the Grüneisen coefficient Γ . In addition, the compressive and tensile contributions to $\sigma_{xx}(x = \delta, t)$, $\sigma_{xx}^-(t - [(\delta + \lambda)/c])$ and $\sigma_{xx}^+(t - [(\delta - \lambda)/c])$, remain separated in time. Thus the measured stress transient yields the distribution of the laser energy within the target since the time variable can be converted to a spatial depth through the propagation velocity c . This demonstrates the use of photoacoustic techniques to measure the distribution of radiation within a medium; providing a means to determine its optical properties. This is shown in figure 2a where tensile and compressive components of the stress transient are exponentials whose rise and decay times scale with the absorption coefficient μ_a .

In the limiting case where the laser pulse duration is much larger than the acoustic transit time, i.e., $\mu_a c t_p \gg 1$, significant particle motion occurs on the time scale of the laser pulse. This has the effect of reducing the maximum uniaxial stress by a factor proportional to μ_a^{-1} [7]. As a result, the magnitude of the laser induced stress is independent of the optical penetration depth and the scaling $\sigma_{xx}(x = \delta) \propto \Gamma \varepsilon''$ applies. Since $1/\mu_a c$ is very small compared to t_p , the compressive and tensile contributions to $\sigma_{xx}(x = \delta)$

Fig. 2a: $\mu_a c t_p \ll 1$

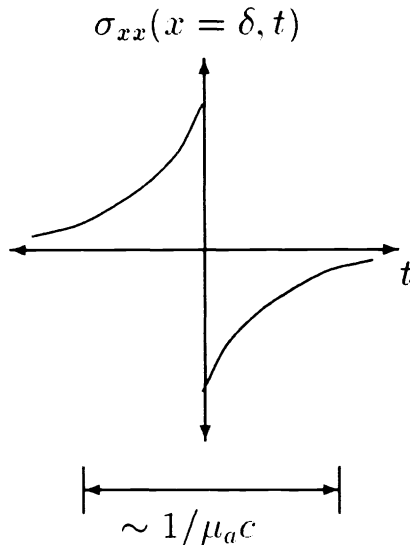


Fig. 2b: $\mu_a c t_p \gg 1$

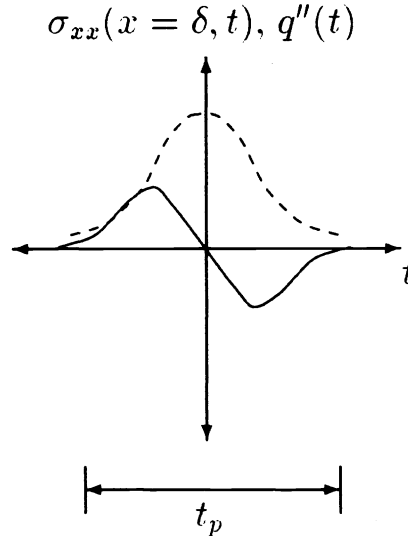


Figure 2: Plot of the stress transients generated in the physical situation considered in figure 1. **(a)** The curve is the shape of the measured stress transient in the case where $\mu_a c t_p \ll 1$. **(b)** The solid curve is the measured stress transient for $\mu_a c t_p \gg 1$ for a Gaussian laser pulse shape (dashed curve).

are no longer separated in time. Instead, the measured stress is the sum of a compressive stress generated at a given time plus a tensile stress generated a brief instant earlier. Since the magnitude of these stresses are proportional to the laser irradiance, the magnitude of the stresses are proportional to the time derivative of the laser irradiance. Accordingly, the duration of the stress transient is simply the duration of the laser pulse, t_p . This is illustrated in figure 2b for a Gaussian pulse shape. With the notable exception of Q-switched Nd:YAG, Q-switched Ho:YAG, and TEA CO₂ laser pulses, most laser sources fall into this case when in the thermoelastic regime.

3 Cavity Formation

There is experimental evidence to indicate that as the radiant exposure increases, mechanical failure of the target may occur, resulting in cavity formation below the tissue surface [12, 14]. The conditions under which the cavity is formed are unclear although possible mechanisms include subsurface vapor formation or localized energy deposition due to inhomogeneous absorption. In any event, once a cavity is formed the absorption of the laser radiation by the material within the cavity leads to an increase in cavity pressure which launches a compressive stress transient. If the laser pulse duration is short compared to the characteristic expansion time of the cavity, the laser-induced stress will reach a maximum at the end of the laser pulse. After the end of the laser pulse mechanical expansion of the cavity and thermal diffusion will relax the internal pressure. Thus the stress transient will be longer than the laser pulse and have a decay time which scales as $t_{decay} \propto 1/\alpha\mu_a^2$, α being the thermal diffusivity of the medium surrounding the cavity. In addition, the peak stress will scale with the volumetric energy deposition $\mu_a \epsilon''$ regardless of the value of $\mu_a c t_p$ so long as the laser pulse duration is short compared to the characteristic thermal diffusion

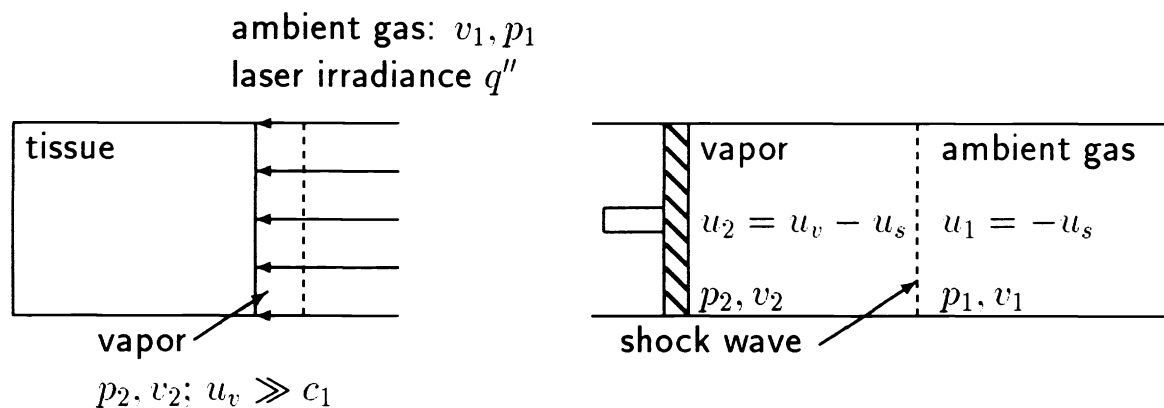


Figure 3: Physical situation considered when determining the recoil stress of the ablation products. The velocities u_1 and u_2 are given in a reference frame moving with the shock wave.

time i.e., $\alpha\mu_a^2 t_p \leq \mathcal{O}(1)$. Stress generation characteristic of cavity formation has been observed to result from pulsed excimer laser irradiation of polyimide [15].

4 Recoil of Ablation Products

At large energy densities strong thermal and acoustic effects are generated within the medium and have the ability to achieve explosive removal of biological tissue. In this case, stress waves are generated by the recoil of the ablation products as well as by the thermoelastic response. However, due to the strong dependence of the recoil stresses on the absorbed radiant exposure, these stresses dominate the thermoelastic stresses at radiant exposures only nominally larger than the ablation threshold.

In order to derive the scaling law for the recoil pressure at the target surface, we will model the ablation process as one of steady vaporization as formulated by Landau and Lifshitz [11]. We consider the one-dimensional case where a layer of vapor at high temperature and pressure is created adjacent to the target surface. We assume the expansion velocity of the vapor u_v to be large compared to the sound velocity in the surrounding medium. This results in the radiation of a shock traveling at velocity u_s . This is shown schematically in figure 3 where we model the vaporization process as a piston moving at a velocity u_v into the surrounding gas. In this case the equations of mass, momentum and energy conservation in a reference frame moving with the shock wave are:

$$\frac{u_1}{v_1} = \frac{u_2}{v_2} = -\dot{m}'' \quad (9)$$

$$p_1 + \frac{u_1^2}{v_1} = p_2 + \frac{u_2^2}{v_2} \quad (10)$$

and

$$h_1 + \frac{u_1^2}{2} = h_2 + \frac{u_2^2}{2} \quad (11)$$

In eqns. (9) and (10), the subscripts '1' and '2' refer to the regions downstream and upstream of the shock wave. Thus region 1 is the surrounding gas under ambient conditions and region 2 consists of a mixture of ablation vapor and ambient gas which has undergone shock compression. h , \dot{m}'' , p , u and v refer to the specific enthalpy, mass flux per unit area, pressure, velocity and specific volume, respectively.

Our goal is to express the vapor flow velocity u_v in terms of the pre- and post- shock pressures p_1 and p_2 . By combining eqns. (9) and (10), we express u_v as a function of the pressures and specific volumes on either side of the shock:

$$u_v = u_2 - u_1 = [(p_2 - p_1)(v_1 - v_2)]^{1/2}. \quad (12)$$

We then combine eqns. (9)–(11) and use the relation $h = pv[\gamma/(\gamma - 1)]$, where γ is the ratio of specific heats c_p/c_v , to relate the ratio of specific volumes across the shock front with the pre- and post- shock pressures:

$$\frac{v_2}{v_1} = \frac{p_1(\gamma_1 + 1) + p_2(\gamma_1 - 1)}{p_1(\gamma_1 - 1) + p_2(\gamma_1 + 1)}. \quad (13)$$

Combining eqns. (12) and (13) we get the following quadratic equation for the compression ratio $\Pi = p_2/p_1$ across the shock:

$$\Pi^2 - \left[2 + \frac{u_v^2 \gamma_1 (\gamma_1 + 1)}{2c_1^2} \right] \Pi + \left[1 - \frac{u_v^2 \gamma_1 (\gamma_1 - 1)}{2c_1^2} \right] = 0, \quad (14)$$

where $c_1 = \sqrt{\gamma_1 p_1 v_1}$ is the adiabatic sound speed in region 1. Solving eqn. (14) for Π and simplifying for the case where $u_v \gg c_1$, we get:

$$\Pi = \frac{\gamma_1 (\gamma_1 + 1) u_v^2}{2c_1^2}. \quad (15)$$

In order to find u_v we apply conservation of energy globally to this process. We assume that the energy necessary to form the vapor is small compared to both the energy which heats the vapor and the work done by the expanding vapor on the surrounding air. In this case energy conservation can be written as:

$$\frac{d\varepsilon}{dt} - \frac{dW}{dt} = q'', \quad (16)$$

where W is the work done by the expanding vapor on the surrounding air per unit surface area and ε is the internal energy of the expanding vapor per unit surface area. Letting z be the thickness of the vapor layer, $W = -p_2 dz$ and $\varepsilon = p_2 z / (\gamma_2 - 1)$. Substituting these expressions into eqn. (16), recognizing that $u_v = (dz/dt)$ and substituting eqn. (15) for p_2/p_1 we get

$$u_v = \left[\frac{2(\gamma_2 - 1)c_1^2 q''}{\gamma_2 \gamma_1 (\gamma_1 + 1) p_1} \right]^{1/3}. \quad (17)$$

Substituting eqn. (17) into (15) and solving for p_2 gives the result:

$$p_2 = \left\{ \left[\frac{\gamma_1 (\gamma_1 + 1) p_1}{2} \right]^{1/2} \frac{(\gamma_2 - 1) q''}{\gamma_2 c_1} \right\}^{2/3}. \quad (18)$$

This result indicates that the recoil stress can be reduced by decreasing the ambient pressure or replacing the ambient gas with one whose adiabatic sound speed is larger (i.e., a gas with lower molecular mass). For those interactions where a steady state ablation process is not achieved due to the short duration of the laser pulse, two changes must be made to the above expression. First, the irradiance q'' should be replaced by the radiant exposure divided by the pulse duration ε''/t_p . Secondly, the amount of energy left in the target (i.e., the threshold radiant exposure for ablation) ε''_{th} should be subtracted from the radiant exposure absorbed by the target. This leads to the following scaling law for the recoil stress [8]:

$$\sigma_{xx} \propto \left[\frac{(\varepsilon'' - \varepsilon''_{th})}{t_p} \right]^{2/3}. \quad (19)$$

Here we see that close to the ablation threshold ε''_{th} the recoil stress increases dramatically with radiant exposure and soon dominates the thermoelastic response which increases only linearly with ε'' .

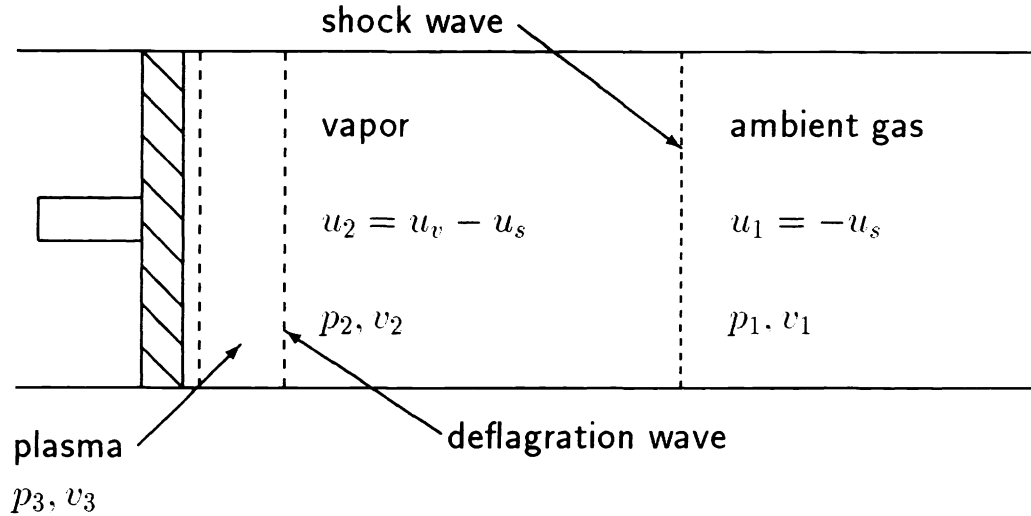


Figure 4: Physical situation considered when determining the recoil effects produced by plasma formation and expansion. The velocities are given in the reference frame of the shock wave. See text for details.

5 Stresses Generated by Plasma Formation and Expansion

At higher energy densities, the irradiance of the laser radiation may be sufficient to ionize the ablation products and form a dense plasma adjacent to the target surface. Since the plasma absorbs a non-negligible portion of the incident laser radiation the gas-dynamics of the ablation flow is altered significantly. Thus the scaling laws derived in the previous section do not apply when plasma mediates the laser-target interaction.

In modeling this situation we again assume that the velocity of the ablation products is much larger than the sound velocity in the ambient gas thereby radiating a shock wave. However, since a portion of the laser energy is also absorbed by the plasma, the shock wave is followed by a deflagration wave which is in turn followed by a rarefaction resulting from the plasma expansion [9]. Figure 4 is a pictorial representation of the physical situation we are considering.

We consider the case where the process of free-free absorption or inverse Bremsstrahlung is the mechanism responsible for plasma heating. This occurs when an electron absorbs a photon thereby moving it from one free state to a more energetic state in the field of an ion. Assuming that the plasma collectively has no net charge, its absorption coefficient μ_a^p in the limit where $h\nu \ll kT_e$ is given by [1]:

$$\mu_a^p = \frac{2}{3\sqrt{6}} \bar{g} \left(\frac{\pi}{m_e k T_e} \right)^{3/2} \frac{n_i^2 Z^3 e^6 \lambda^2}{\epsilon_0^3 c^3}, \quad (20)$$

where

c – speed of light, $= 2.99792 \times 10^8 \text{ ms}^{-1}$,

e – proton charge, $= 1.60219 \times 10^{-19} \text{ C}$,

\bar{g} – Gaunt factor, [-],

\hbar – $h/2\pi$, $= 1.05459 \times 10^{-34} \text{ Js}$,

k – Boltzmann constant, $= 1.38066 \times 10^{-23} \text{ JK}^{-1}$,

m_e – electron mass, $= 9.10953 \times 10^{-31} \text{ kg}$,

n_i – ion density, $[\text{m}^{-3}]$,

T_e – electron temperature, $[\text{K}]$,

Z - atomic number, [-],
 ϵ_0 - permittivity of free space, = $8.85419 \times 10^{-12} \text{ C}^2\text{J}^{-1}\text{m}^{-1}$,
 λ - laser wavelength, [m] and
 ν - laser frequency, [s^{-1}].

The specific volume and sound speed of the plasma, v_3 and c_3 , are given by:

$$v_3 = \frac{Z}{Am_p n_e} \quad \text{and} \quad c_3 = \left[\frac{(Z+1)\gamma_3 k T_3}{Am_p} \right]^{1/2}, \quad (21)$$

where

A - mass number, [-],
 n_e - electron density, [m^{-3}] and
 m_p - proton mass, = $1.67265 \times 10^{-27} \text{ kg}$.

These equations permit the expression of the plasma absorption coefficient in terms of the hydrodynamic variables:

$$\mu_a^p = \frac{\Xi}{v_3^2 c_3^3}, \quad (22)$$

where

$$\Xi = \bar{g} \frac{Z^3 (Z+1)^{\frac{3}{2}} \gamma^{\frac{3}{2}} \pi^{\frac{3}{2}} \lambda^2 \epsilon^6}{3\sqrt{6} A^{\frac{7}{2}} m_p^2 m_e^{\frac{3}{2}} \epsilon_0^3 c^3}. \quad (23)$$

We assume that the Chapman-Jouget condition is satisfied and the plasma expands at the speed of sound in the adjacent medium. This gives us the following upper bound on the optical thickness of the plasma \mathcal{S} :

$$\mathcal{S} = \mu_a^p c_2 t. \quad (24)$$

We assume that the optical thickness $\mathcal{S} = \mathcal{O}(1)$ since if the plasma is transparent (i.e., $\mathcal{S} < \mathcal{O}(1)$), the heating rate of the plasma will be small and will lead to an increase in both the rate of target vaporization and the optical thickness of the plasma. Conversely, if the plasma is optically thick ($\mathcal{S} > \mathcal{O}(1)$), the target will be shielded by the plasma and will lead to a decrease in both the rate of vaporization and the optical thickness of the plasma. Thus there exists an ‘equilibrium’ optical thickness of the plasma where the rate of expansion of the plasma is compensated by the supply of ionized ablation products through vaporization. Such a situation is referred to as the “self-matched regime” after Krokhin [10]. Next, we need to determine the relation between the velocity of the plasma expansion and the laser irradiance q'' . We assume that a negligible amount of energy is necessary for vaporization and ionization of the target and that the ablation products are sufficiently characterized as an ideal gas. In this case it can be shown from energy conservation that the irradiance is related to the velocity of the ablative flow through the relation [9]:

$$q'' = \frac{c_2^3}{v_2} \left[\frac{M_2}{2} (M_2^2 + 3) \right], \quad (25)$$

where M_2 is the Mach number = u_2/c_2 . Solving for v_2 and c_2 from eqns. (22), (24) and (25) we get the following scaling laws:

$$v_2 \propto \left(\frac{\Phi}{q''} \right)^{1/4} \left(\frac{\Xi t}{\mathcal{S}} \right)^{3/8} \quad \text{and} \quad c_2 = \left(\frac{q''}{\Phi} \right)^{1/4} \left(\frac{\Xi t}{\mathcal{S}} \right)^{1/8}. \quad (26)$$

where $\Phi = M_2(M_2^2 + 3)/2$. Thus the pressure developed within the plasma due to laser heating is given by the scaling law:

$$p_2 \propto \left(\frac{\mathcal{S}}{\Xi t}\right)^{1/8} \left(\frac{q''}{\Phi}\right)^{3/4}. \quad (27)$$

Since the recoil stress at the target surface differs only by a multiplicative factor dependent on the plasma characteristics, this scaling law also applies to the recoil stress at the target surface σ_{xx} . This result shows that although the plasma mediates the interaction, the dependence of the recoil stress on the optical thickness is very weak. This shows that our assumption that the optical thickness be $\mathcal{O}(1)$ is not critical to the final result. In addition, we find that although less energy is coupled into the target for plasma mediated interactions, the recoil stress is more strongly dependent on the incident irradiance.

6 Summary and Conclusions

In this paper we have considered the character of the stress transients generated by thermoelastic expansion, cavity formation, ablative recoil and plasma formation and expansion. The results indicate that the stresses generated by each of these mechanisms display unique characteristics with regards to their temporal behavior and with the scaling of their magnitudes with laser and material parameters. We have shown that photoacoustic measurement techniques have the potential to determine the optical properties of a medium. We have also shown that the recoil stresses associated with ablation rise very sharply with increasing radiant exposure when close to the ablation threshold. Thus in the ablative regime, a reduction in the recoil stress can be achieved with a lower pulse energy. Alternatively, the recoil stress can be reduced if the ambient pressure is reduced or if an ambient gas with lower molecular mass is used. When ionization of the ablation products occurs, the scaling of the recoil stress with the incident radiant exposure is stronger than when plasma is not present.

As interest in the effect of laser-induced stresses on biological systems increases, it is of prime importance to characterize the stress transients to which these system will be exposed. To this end, it is hoped that the framework presented here will aid in the design of such studies.

Acknowledgments: The authors thank Mariano E. Gurfinkel Castillo for many helpful discussions and for general assistance in the preparation of this manuscript. This work was sponsored by the Medical Free Electron Laser program of the Strategic Defense Initiative Organization under contract N00014-91-C-0017.

References

- [1] C. W. Allen. *Astrophysical Quantities*. Athlone, London, 3rd edition, 1973.
- [2] E. F. Carome, N. A. Clark, and C. E. Moeller. Generation of acoustic signals in liquids by ruby laser-induced thermal stress transients. *Appl. Phys. Lett.*, 4(6):95–97, March 1964.
- [3] A. G. Doukas, D. J. McAuliffe, and T. J. Flotte. Biological effects of laser-induced shock waves: structural and functional damage *in vitro*. *Ultrasound in Med. and Biol.*, To appear.
- [4] P. E. Dyer and R. K. Al-Dhahir. Transient photoacoustic studies of laser tissue ablation. *SPIE*, 1202:46–60, 1990.
- [5] P. E. Dyer and R. Srinivasan. Nanosecond photoacoustic studies on ultraviolet laser ablation of organic polymers. *Appl. Phys. Lett.*, 48(6):445–447, 1986.

- [6] T. J. Flotte. Personal communication.
- [7] L. S. Gournay. Conversion of electromagnetic to acoustic energy by surface heating. *J. Acoust. Soc. Am.*, 40(6):1322–1330, 1966.
- [8] R. D. Griffin, B. L. Justus, A. J. Campillo, and L. S. Goldberg. Interferometric studies of the pressure of a confined laser-heated plasma. *J. Appl. Phys.*, 59(6):1968–1971, January 1986.
- [9] R. E. Kidder. Application of lasers to the production of high-temperature and high-pressure plasma. *Nucl. Fusion*, 8:3–12, 1968.
- [10] O. N. Krokhin. ‘Matched’ plasma heating mode using laser radiation. *Sov. Phys. Tech. Phys.*, 9(5):1024–1026, 1965.
- [11] L. D. Landau and E. M. Lifshitz. *Fluid Mechanics*. Pergamon Press, Oxford, 2nd edition, 1987.
- [12] G. L. LeCarpentier, M. Motamedi, and A. J. Welch. Effects of pressure rise on cw laser ablation of tissue. *SPIE*, 1427:273–278, 1991.
- [13] A. E. H. Love. *A Treatise on the Mathematical Theory of Elasticity*. Dover Publications, New York, 1944.
- [14] R. M. Verdaasdonk, C. Borst, and M. J. C. van Gemert. Explosive onset of continuous wave laser tissue ablation. *Phys. Med. Biol.*, 35(8):1129–1144, 1990.
- [15] A. D. Zweig, V. Venugopalan, and T. F. Deutsch. A study of the pressure transients produced by pulsed excimer-laser irradiation of polyimide. *Submitted to J. Appl. Phys.*, October 1992.